Clinical and Translational Report

Cell Metabolism

# The Gut Microbiota Regulates Intestinal CD4 T Cells Expressing RORγt and Controls Metabolic Disease

## Graphical Abstract

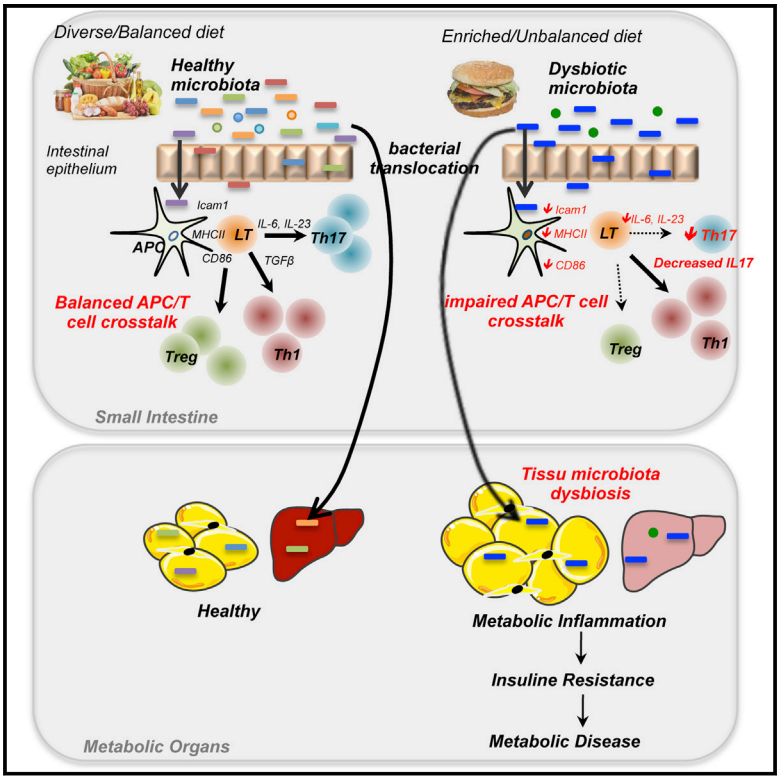


## Authors

Lucile Garidou, Céline Pomié, Pascale Klopp, ..., Victorine Douin-Echinard, Christophe Heymes, Rémy Burcelin

## Correspondence

lucile.garidou@gmail.com (L.G.), remy.burcelin@inserm.fr (R.B.)

## In Brief

Obesity and type 2 diabetes have been linked to the gut microbiota. Garidou et al. show that a high-fat diet induces gut microbiota dysbiosis which impairs the intestinal immune defense, including reduced intestinal IL 17 T cells. The intestinal immunity changes precede the onset of diabetes.

## Highlights

- HFD-induced T2D decreases the number of ileum IL17/RORγt CD4 T cells
- IL17/RORγt-deficient CD4 T cells induce T2D and obesity
- HFD-induced ileum microbiota dysbiosis lowers intestinal IL17/RORγt-CD4 T cells
- HFD reduces antigen presenting cell ability to induce Th17 cell differentiation

## Accession Numbers

GSE52557
GSE52558
GSE52559

Garidou et al., 2015, Cell Metabolism 22, 100–112
July 7, 2015 
http://dx.doi.org/10.1016/j.cmet.2015.06.001

CellPress

CellPress

Cell Metabolism
Clinical and Translational Report

# The Gut Microbiota Regulates Intestinal CD4 T Cells Expressing RORγt and Controls Metabolic Disease

Lucile Garidou,[1,2,10,*] Céline Pomié,[1,2,10] Pascale Klopp,[1,2] Aurélie Waget,[1,2] Julie Charpentier,[1,2] Meryem Aloulou,[2,3,4] Anaïs Giry,[1,2] Matteo Serino,[1,2] Lotta Stenman,[5] Sampo Lahtinen,[5] Cedric Dray,[1,2] Jason S. Iacovoni,[6] Michael Courtney,[7] Xavier Collet,[1,2] Jacques Amar,[2,8] Florence Servant,[7] Benjamin Lelouvier,[7] Philippe Valet,[1,2] Gérard Eberl,[9] Nicolas Fazilleau,[2,3,4] Victorine Douin-Echinard,[1,2] Christophe Heymes,[1,2] and Rémy Burcelin[1,2,*]

[1]Institut des Maladies Métaboliques et Cardiovasculaires, INSERM U1048 F-31432 Toulouse, France
[2]Université Paul Sabatier, F-31432 Toulouse, France
[3]Centre de Physiopathologie de Toulouse Purpan, INSERM U1043, F-31300 Toulouse, France
[4]CNRS, UMR5282, F-31300 Toulouse, France
[5]Danisco Sweeteners Oy Sokeritehtaantie 20 FI-02460 Kantvik, Finland
[6]Plateau de Bioinformatique et Biostatistique, INSERM UMR1048, F-31432 Toulouse, France
[7]Vaiomer SAS, 516 Rue Pierre et Marie Curie, F-31670 Labège, France
[8]Hôpital Rangueil, Département Thérapeutique, F-31059 Toulouse, France
[9]Institut Pasteur, Unité de Développement des Tissus Lymphoïdes, F-75724 Paris, France
[10]Co-first author
*Correspondence: lucile.garidou@gmail.com (L.G.), remy.burcelin@inserm.fr (R.B.)
http://dx.doi.org/10.1016/j.cmet.2015.06.001

## SUMMARY

**A high-fat diet (HFD) induces metabolic disease and low-grade metabolic inflammation in response to changes in the intestinal microbiota through as-yet-unknown mechanisms. Here, we show that a HFD-derived ileum microbiota is responsible for a decrease in Th17 cells of the *lamina propria* in axenic colonized mice. The HFD also changed the expression profiles of intestinal antigen-presenting cells and their ability to generate Th17 cells in vitro. Consistent with these data, the metabolic phenotype was mimicked in RORγt-deficient mice, which lack IL17 and IL22 function, and in the adoptive transfer experiment of T cells from RORγt-deficient mice into Rag1-deficient mice. We conclude that the microbiota of the ileum regulates Th17 cell homeostasis in the small intestine and determines the outcome of metabolic disease.**

## INTRODUCTION

A major feature of type 2 diabetes (T2D) is the inability of peripheral tissues to adequately respond to insulin (termed insulin resistance). This metabolic disease is characterized by systemic low-grade inflammation of liver, muscle, and adipose tissue (AT), referred to as metabolic inflammation (Hotamisligil, 2006).

T2D can be induced in mice genetically or by a high-fat diet (HFD), which also induces production of the inflammatory cytokines, interleukin (IL) 1β, and TNFα and chemokine CCL2 in mesenteric AT (MAT) (Weisberg et al., 2003). Moreover, AT infiltration by T and B cells increases the inflammatory state in obese mice, leading to insulin resistance (Nishimura et al., 2009; Winer et al., 2011). Loss-of-function experiments demonstrated an imbalance between regulatory and effector T cells which is crucial in this inflammation (Feuerer et al., 2009).

Results from our laboratory (Cani et al., 2008) and others (Turnbaugh et al., 2006) have demonstrated that obesity and T2D are associated with an increase in the ratio of *Firmicutes* to *Bacteroidetes* phyla in the gut microbiota. These changes are associated with increased energy harvesting and upregulation of genes implicated in hepatic lipogenesis and AT development (Bäckhed et al., 2004; Turnbaugh et al., 2006). Another way in which changes in the gut microbiota might induce low-grade inflammation is by modulation of the gut immune system (Atarashi et al., 2011; Ivanov and Littman, 2011), including cells of both the innate (macrophages, dendritic cells, and innate lymphoid cells) and the adaptive immune systems.

In the gut, CD4 T cells contribute to immunity by differentiating into various subsets, notably inflammatory and regulatory cells (Bollrath and Powrie, 2013; Shale et al., 2013). Th17 cells are the most abundant CD4 T cells in mucosal tissues (Littman and Rudensky, 2010). They secrete two isoforms of IL17 (IL17A, IL17F) and/or IL22, which confer protection against fungi and pathogenic bacteria. Th17 cell differentiation is mediated by the transcription factor retinoid-related orphan receptor gamma t (RORγt) (Ivanov et al., 2006), and induced by cytokines: TGFβ1, IL6, IL1β and IL21, and maintained by IL23 (Chewning and Weaver, 2014).

The development and maturation of the immune system is influenced by gut microbiota (Hooper and Gordon, 2001; Sommer and Bäckhed, 2013). Some commensal bacteria, such as segmented filamentous bacteria (SFB), are necessary for gut Th17 cell development (Gaboriau-Routhiau et al., 2009; Ivanov et al., 2009). In contrast, *Clostridium* and *Bacteroides fragilis* favor Tregs development (Atarashi et al., 2011; Round and Mazmanian, 2010). We hypothesized that changes in the gut immune system, in response to changes in gut microbiota, would be sufficient to trigger metabolic disease like T2D. In this study, we set out to test this hypothesis by analyzing the changes in intestinal T cells induced by feeding mice with a HFD and demonstrated their causal role through T cell adoptive transfer. We further

report evidences that dysbiotic ileum microbiota impart changes in intestinal innate immune and CD4 T cell homeostasis—notably, a loss of Th17 cells. These changes precede the onset of metabolic disease, and they are sufficient to induce glucose intolerance and insulin resistance features of T2D.

## RESULTS AND DISCUSSION

### HFD-Induced T2D Impairs Intestinal Immunity

To investigate how the gut immune system is affected at the earliest stages of diet-induced metabolic disease, we studied a first animal model in which the mice were fed a fat-enriched, carbohydrate-free diet for 10 or for 30 days. After 10 and 30 days on HFD, the mice were glucose intolerant and insulin resistant, but their fasting glycemia levels were not different from that of normal chow (NC)-fed mice (NC) (Figures 1A and 1B). The liver triglyceride concentration was not different when compared to NC-fed mice (see Figure S1A available online) but later accumulates at 3 months of HFD (Burcelin et al., 2002). This animal model is also characterized by a strong lipotoxicity, since the mice are insulinopenic, as shown in the fed state (Figure S1B). Consequently, the fed plasma insulin/glucose ratio was reduced in the HFD-fed mice (Figure S1C). Due to this relative hypoinsulinemic state, the mice did not gain significant weight during this short period of time, although the HFD-fed mice had a higher fat/lean ratio than the control mice (Figures S1D and S1E). However, over 3–6 months the HFD-fed mice adapt to the diet and eventually gain significant weight (Burcelin et al., 2002). Altogether, studying mice fed a 72% HFD avoids the confounding effects of obesity on glucose tolerance and insulin resistance. In contrast to previous reports (Bleau et al., 2014), the subcutaneous AT and MAT mRNA levels for inflammatory cytokines (TNF$\alpha$, IFN$\gamma$, IL6, and PAI1) were not significantly different after 10 and 30 days on HFD when compared to NC mice (Figures S1F and S1G). This is most likely due to the fact that we studied the early onset of the disease, suggesting that the metabolic inflammation observed by others could be the consequence of hyperglycemia and excessive body weight gain. This conclusion is further supported by our data since no change in IL17A, IL17F, and IL22 mRNA levels was observed at the onset of HFD-induced metabolic disease (Figures S1F and S1G). To better define this issue, we quantified cell number from the MAT and observed a slight increase of IL17-producing CD4 T cells (Th17) after 10 days on HFD when compared to NC mice (Figure S1H). Foxp3-expressing regulatory T (Treg) cell number was transiently decreased after 10 days on HFD mice when compared to NC mice (Figure S1I). IFN$\gamma$-producing CD4 T cell number (Th1) was not affected by the HFD (Figure S1J). In summary, no major inflammatory process was observed in the MAT after only 30 days on HFD. In the liver, a major site of HFD-induced metabolic inflammation, mRNA levels of IL17A and IL17F were increased from 10 days of HFD (Figure S1K). Second, the number of Th17 cells in the liver was increased after 10 days on HFD and remained statistically elevated after 30 days on HFD compared to NC mice (Figure S1L). Furthermore, Treg cell number was slightly decreased from 10 days on HFD when compared to NC mice (Figure S1M), and Th1 cell number decreased transiently after 10 days and returned to the same level as NC after 30 days on HFD (Figure S1N). Eventually, the p-NF$\kappa$B to NF$\kappa$B ratio was increased after 30 days on HFD (Figure S1O). Altogether, we observed moderate inflammation in the liver related to Th17 cells in response to the HFD at the onset of metabolic disease. In the quest of a major tissue responsible for the late development of tissue inflammation and consequently metabolic disease, we evaluated changes in intestinal cytokine production at the onset of metabolic disease. In the ileum and in Peyer's patches, IL22, IL17A, IL17F, and IL10 mRNA levels were decreased in HFD (Figure S1P and S1Q) when compared to controls. Similarly, in the MLN, IL17A and IL22 mRNA levels decreased dramatically after 10 days and remained low after 30 days on HFD despite the slight increase of IFN$\gamma$ and PAI1 mRNA levels (Figure S1R). In the colon of HFD mice, the IL22 and IL10 mRNA levels were decreased, IL17A was not detectable, and no major change was noticed in IL17F despite a small increase of IFN$\gamma$ and IL6 mRNA levels (Figure S1S). This suggests a loss of IL17- and IL22-secreting cells, which is rather a feature of a reduced inflammatory process. Since the most dramatic changes in cytokine expression were in the ileum rather than in the colon, we focused the rest of our study on the small intestine (SI) and observed first, in the *lamina propria* (the subepithelial layer) of the SI (SILP), that the proportion and number of Th17 cells were decreased after 10 and 30 days on HFD when compared to the NC (Figures 1C and 1D). This is consistent with the reduction in IL17 mRNA levels already mentioned (Figure S1P). We also found a decrease in the proportion and number of ROR$\gamma$t-expressing CD4 T cells after 30 days on HFD (Figures 1E and 1F). Second, we found that Tregs decreased in proportion and number in the SILP after 30 days on HFD (Figures 1G and 1H). Third, we quantified the Th1 cells and found their proportion increased in the SILP after 30 days on HFD compared to the NC, although both contained a similar number of Th1 cells (Figures 1I and 1J), which may be explained by the decrease in total T cell number (Figure S1T). Therefore, our data show a moderated increased proportion of Th1 cells at the onset of the disease which remains further sustained later, as reported elsewhere (Luck et al., 2015). Importantly, our present data further show a reduced number of intestinal Th17 cells at the onset which defined a low state of inflammation, whereas recent data show that HFD induced an increased intestinal inflammatory state at later stage of the disease. Altogether, both sets of data suggest that metabolic disease is the consequence of first a reduced intestinal inflammation, as characterized by a low number of Th17 cells. Second, intestinal inflammation develops at a late stage of the disease (Luck et al., 2015).The origin of the late-stage intestinal inflammation is yet unknown.

Moreover, no Th2 cells (IL4-producing CD4 T cells) were detected (data not shown), and we found no changes in Th17, Tregs, Th1, and Th2 cells in the intraepithelial layer (IEL; the layer facing the lumen) (Figures S1U–S1W) or in the MLN (Figures S1X–S1Z).To rule out any contribution of MLN, we surgically ablated those lymph nodes. These mice developed glucose intolerance to the same extent as sham-operated mice (data not shown), suggesting that the changes observed were specific to the SILP.

Taken together, T cell subset analyses indicate a loss of Th17 cells and Tregs specifically in the SILP at the onset of metabolic disease. We then repeated these findings in another model of metabolic disease associated with obesity, high-fat high-carbohydrate diet (HFHCD) fed mice. After 1 month of a HFHCD, mice

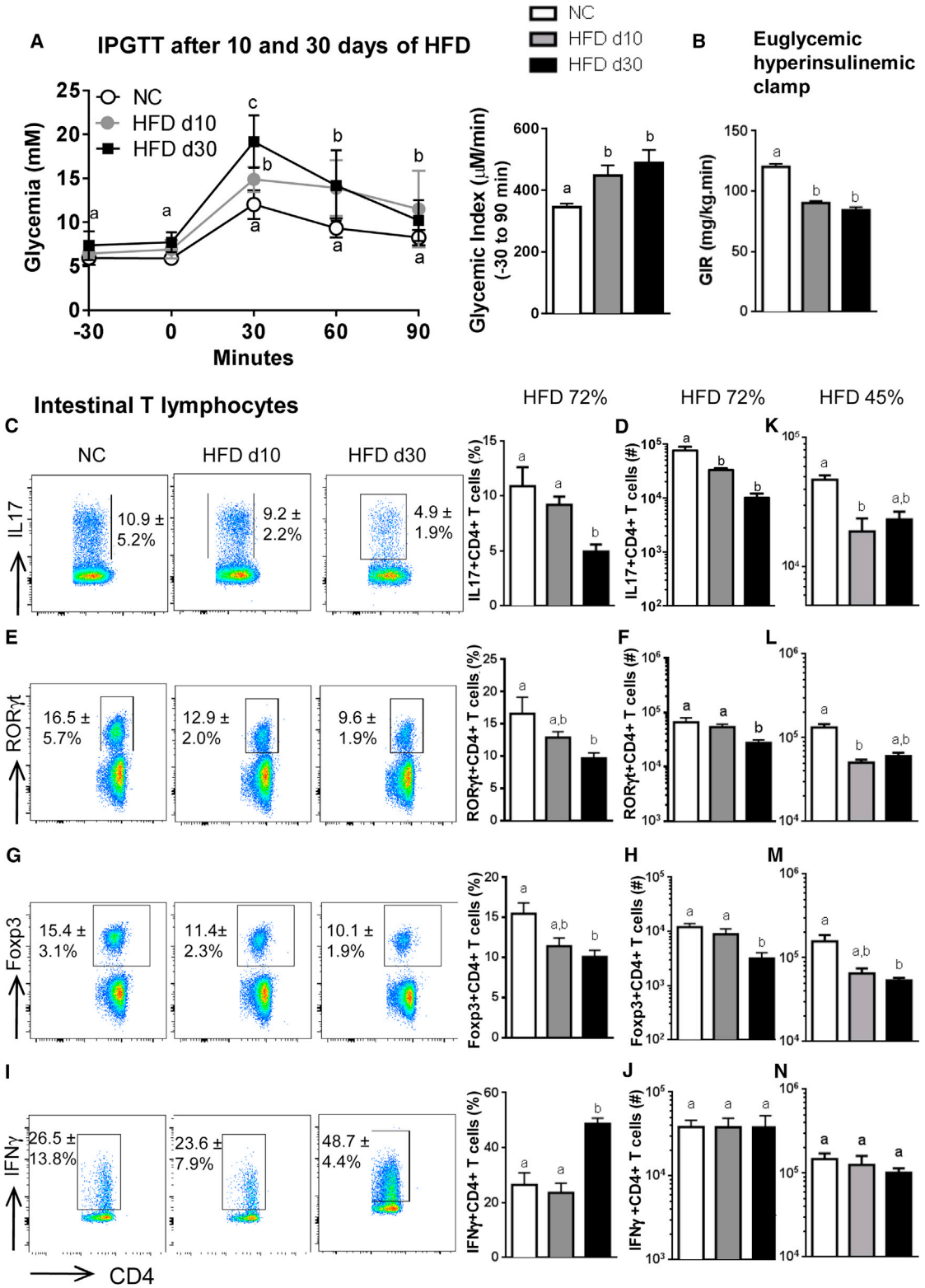


**Figure 1. The HFD Induces Changes in Intestinal Immunity before the Onset of Insulin Resistance**

(A–J) Mice were fed a NC or a HFD 72% for 10 or 30 days.

(K–N) Mice were fed a NC or a HFHCD (45%) for 10 or 30 days.

(A) IPGTT was performed on WT mice fed with a NC or fed a HFD for 10 (HFD d10) or 30 days (HFD d30). The glycemic index (µM/min) was calculated as described in the Experimental Procedures. Graphs show mean ± SEM; n = 5 mice/group; data are from one experiment out of three.

*(legend continued on next page)*

became glucose intolerant (Figure S2A) and obese (Figures S2B and S2C). The number of T cells in the SILP was also reduced after 10 and 30 days on the HFHCD (Figure S2D). The number of Th17 and Treg cells was also decreased in the SILP after 10 and 30 days on the HFHCD (Figures 1K–1M) and the number of Th1 unaffected (Figure 1N).

Altogether, the above data show that a HFD, irrespective of the presence of carbohydrate, induces a strong specific decrease in the number of Th17 cells within the SILP which may lead to the onset of metabolic disease. It is noteworthy that T2D patients are more sensitive than normal to intestinal infections with pathogens like *Candida guilliermondii*, further suggesting that they may have impaired Th17 cells (Khovidhunkit et al., 2009; Lutsey et al., 2009; Macêdo et al., 2010). Consistent with this observation in human subjects, it was shown that HFD-fed rodents were more prone to *Candida albicans* infection than controls (Lefèvre et al., 2010). This was attributed to a shift of cecal APCs/macrophages toward an anti-inflammatory profile in the HFD-fed mice.

## IL17/RORγt-Deficient CD4 T Cells Induce T2D and Obesity

To determine whether the reduced RORγt/Th17 seen in the SILP in response to the HFD is linked to the onset of metabolic disease, we investigated mice lacking RORγt. When 20-week-old, RORγt knockout (*RORγt*$^{-/-}$) mice fed a NC diet became glucose intolerant, hyperinsulinemic, and slightly insulin resistant (Figures 2A–2C) and gained more weight than the WT mice (Figures 2D and 2E) No statistic differences in food intake and hepatic triglyceride concentration were detected (Figures 2F and S3A).

Of note, *RORγt*$^{-/-}$ mice fed the HFD rapidly lost weight and died within one month (data not shown). This could be due to a deleterious effect of the lipotoxicity induced by the HFD. In addition to the lipotoxicity, the changes in gut microbiota induced by the HFD (Cani et al., 2008) could lead to an immunological stress in *RORγt*$^{-/-}$ mice, which lack secondary lymphoid organs, which has previously been associated with excessive bacterial burden leading to death (Lochner et al., 2011). This important phenotype is still under investigation. We then studied heterozygous *RORγt*$^{+/-}$ mice. First, 12-week-old heterozygous *RORγt*$^{+/-}$ mice were slightly glucose intolerant (Figure 2G) and obese (data not shown). Insulin sensitivity was slightly reduced when compared to WT mice (Figure 2H), suggesting that the lack of one allele of RORγt is a risk factor for metabolic disease. Second, we challenged the mice with a HFD (72% fat). After 30 days, the *RORγt*$^{+/-}$ mice became more glucose intolerant, had more fat mass and were insulin resistant than WT mice (Figures 2H–2J). The difference in fat mass accumulation is most likely due to a slight increase in food intake. However, we cannot rule out that reduced energy expenditure could also be involved, since the deficient mice were slightly insulin resistant. This latter trait is often associated with reduced energy expenditure. Altogether, RORγt-deficient mice develop metabolic disease.

To determine whether the metabolic phenotypes of the RORγt-deficient mice correlated with the status of their CD4 T cell subsets in the SILP, we analyzed T cell populations. As expected in *RORγt*$^{-/-}$ mice, no Th17 cells were detected (Ivanov et al., 2006), whereas Tregs and Th1 cells were found in similar proportions (Figures 2K–2M). In *RORγt*$^{+/-}$ mice fed NC, the proportion of Th17 and Treg cells in the SILP was reduced by about half when compared to WT mice (Figures 2N and 2O). Conversely, the proportion of Th1 cells was higher in the *RORγt*$^{+/-}$ mice fed NC than in WT mice. No additional effect of the HFD was observed (Figure 2P). Th2 cells were not detected in the SILP of *RORγt*$^{+/-}$ mice (data not shown). Together, the decrease of IL17/RORγt CD4 T cells in the SILP is strongly associated with the development of T2D, confirming the importance of these cells in the control of metabolic disease.

To demonstrate that the absence of IL17/RORγt in T cells rather than in innate lymphoid cells is crucial in the development of metabolic disease, *Rag1*$^{-/-}$ mice were injected with splenic T cells isolated from *RORγt*$^{-/-}$ or WT mice. The *Rag1*$^{-/-}$ mice, which lack T and B cells, were injected with T cells from *RORγt*$^{-/-}$ mice and were more glucose intolerant, insulin resistant, and hyperinsulinemic (Figures 2Q–2S) than did those injected with T cells from WT mice. In addition, the decreased insulin responsiveness was supported by the reduced phosphorylation of Akt and GSK3 in the liver and muscles (EDL and soleus) (Figures 2T–2V). Furthermore, the *Rag1*$^{-/-}$ mice injected with *RORγt*$^{-/-}$ T cells gained more weight than the control, but no differences in food intake and hepatic triglyceride accumulation were observed (Figures 2W–2Y and S3B).

Altogether, this set of data further suggests that IL17/RORγt T cells are key players in the control of metabolic disease, ruling out other IL17- and IL22-producing cells such as innate lymphoid cells and γδ T cells. In agreement with our findings on RORγt-expressing cells, a recent study demonstrated the role of IL22 in the control of metabolic disease through its positive action on AT, liver, and muscle metabolism. This study suggests a role for the immunity of the colon in the control of metabolism (Wang et al., 2014). In our study, we further suggest that IL17, in the control of metabolism, originates from RORγt CD4 T cells of the small intestine, rather than of the colon. These differences could also be related to the the HFD exposure, since this decrease of the number of RORγt/Th17 cells is observed as soon as the onset of HFD-induced insulin resistance and glucose intolerance. To further investigate this hypothesis, we performed a gain of function by increasing IL17-expressing cells in the intestine in HFD-treated mice, using dextran sodium sulfate (DSS) (Figure S4A). This experimental procedure generates an intestinal inflammation through a mechanism involving an increased gut permeability to bacteria, which is associated with an elevated IL17 production (Konieczna et al., 2013). Pretreatment of mice with DSS prevented HFD-induced glucose intolerance and insulinopenia (Figures S4B and S4C). Body weight gain

(B) Glucose infusion rate (GIR) was calculated during euglycemic hyperinsulinemic clamp in NC or HFD-fed mice (n = 8 mice/group).
(C–N) SILP leukocytes (CD4$^+$TCR$^+$CD45$^+$ cells) from mice fed a NC diet, a HFD, or a HFHCD were analyzed by flow cytometry. The boxed population shows proportion of CD4 T cells and is represented in histogram (n = 5 mice/group; data from 1 experiment out of 4). (C, D, and K) Proportion (%) (C) and number (#) (D and K) of IL17$^+$ CD4 T cells after stimulation. (E, F, and L) Proportion (%) (E) and number (#) (F and L) of SILP RORγt$^+$ CD4 T cells. (G, H, and M) Proportion (%) (G) and number (#) (H and M) of Foxp3 Treg cells. (I, J, and N). Proportion (%) (I) and number (#) (J and N) of IFNγ$^+$ CD4 T cells upon stimulation. Graphs show mean ± SEM; Different superscript letters (a,b) in each graph indicate data statistically different with $p > 0.05$.

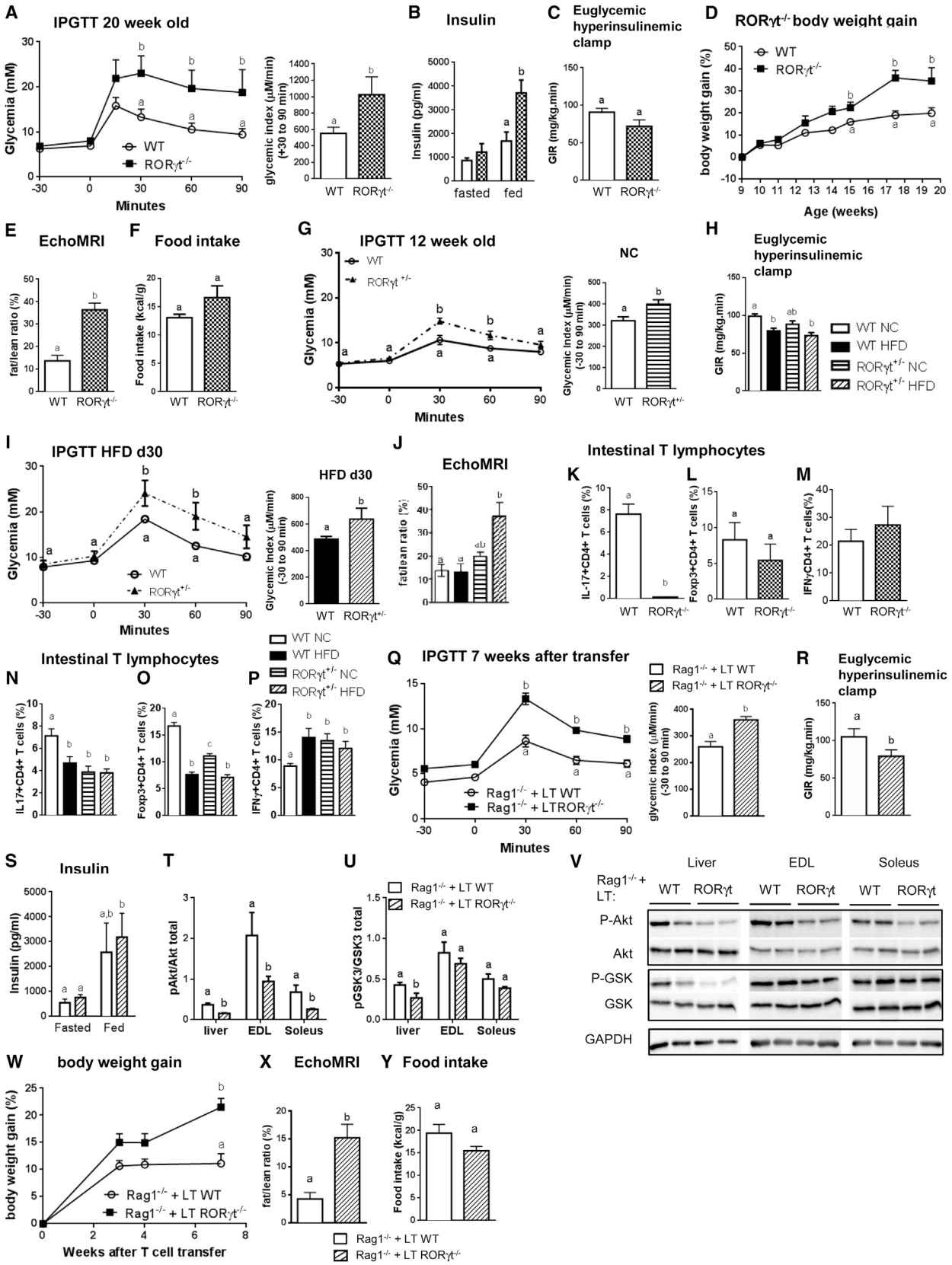


*(legend on next page)*

and food intake remained unchanged (Figure S4D; data not shown). The prevention from HFD-induced glucose intolerance was associated with an increase of IL17A and IL22 mRNAs in the ileum, as expected (Figures S4E and S4F). However, we cannot rule out an independent role of a change in gut microbiota induced by the DSS treatment, which could also increase the number of Th17-producing cells and be responsible for the prevention of HFD-induced metabolic disease. Altogether, this set of data suggests that the maintenance of a steady intestinal inflammatory tone prevents from the later impact of a risk factor, such as HFD, on metabolic disease. This conclusion is supported by a study showing that mice deficient in the TGFβ-activating kinase TAK1 spontaneously develop inflammation of the ileum and are resistant to metabolic disease (Kang et al., 2011). Likewise, the incidence of metabolic disease is lower in humans with intestinal inflammatory syndrome than it is in the general population (Brown et al., 2012). Overall, these experiments in which Th17 cell function is either lost (as in *RORγt*$^{-/-}$ mice) or gained (as in inflammatory conditions) demonstrate that intestinal RORγt/Th17 cells play an important role in the onset of HFD-induced metabolic disease.

### HFD Changes Intestinal Microbiota which Affects Intestinal IL17/RORγt-Expressing CD4 T Cells

It is well accepted that the HFD modulates the gut microbiota (Turnbaugh et al., 2006) and leads to the development of metabolic disease. To evaluate whether this microbiota dysbiosis is responsible for the loss of intestinal Th17 cells in response to the HFD, we first monitored the changes in the gut microbiota by 16S rRNA gene sequencing of the ileum mucosa. Concomitant with the loss of Th17 cells, the microbial composition of the ileum mucosa after 10 and 30 days on HFD changed drastically when compared to NC mice (Figure 3A). This result was confirmed in feces (data not shown). The relative abundance of the *Porphyromonadaceae* decreased after 10 days, whereas that of *Bacteroidaceae* and *Comamonadaceae* increased (Figures 3B, S5A, and S5B) and the proportion of the *Helibocateraceae* and *Peptostreptococcaceae* increased after 30 days on HFD. Additionally, we also confirmed changes in ileum microbiota associated with the decrease of IL17/RORγt cells with the HFHCD-fed mouse model (Figures 1K, 1L, S5C, and S5D).

To investigate that the decreased number of intestinal Th17 cells observed in HFD-induced metabolic disease was due to the intestinal dysbiosis itself and not to the fat in the diet, we treated HFD-fed mice daily by oral gavage with a mixture of prebiotic and probiotic. As expected, this synbiotic treatment (Kolida and Gibson, 2011) profoundly affected the ileum mucosa microbiota (Figures 3C and 3D). 16S rRNA gene sequencing analysis revealed that HFD-fed mice given the synbiotic treatment had a microbiota distinguishable from the other groups (Figure 3C). We observed an increase in *Sutterellaceae*, *Coriobacteriaceae* and *Bacteroidaceae*, and a decrease in *Lachnospiraceae* in comparison to WT NC and HFD mice (Figures 3D, S5A, and S5B). Furthermore, the synbiotic treatment reversed the decrease in *Porphyromonadaceae* and the increase in *Peptostreptococcaceae* and *Comamonadaceae,* seen in HFD mice. The change of microbiota, after 30 days of HFD, in synbiotic-treated mice was associated with an improved glucose tolerance (Figure 3E) and fat/lean ratio (Figure S5E). Similarly, insulin secretion was modestly improved along with the normalization of the plasma insulin to glycemia concentration ratio (Figures S5F ans S5G), and insulin resistance was also reduced when compared to HFD mice (Figure 3F). However, no significant differences in food intake, body weight, and hepatic triglyceride concentrations were induced by the synbiotic (Figures S5H–S5J). The metabolic improvement due to synbiotic treatment was associated with the prevention of decrease in numbers of Th17 and Treg cells in the SILP, without affecting their Th1 number (Figures 3G–3I). Altogether, our results showed that synbiotic treatment modulated the gut microbiota and provided some protection from the effect of 30 days HFD through improved glucose tolerance and prevention of the loss of Th17 cells within the SILP. Furthermore, the frequency of bacteria families, *Porphyromonadaceae*, *Peptostretococaceae*, *Comamonadaceae*, and *Bacteroidaceae* correlates with the ileum IL17 and RORγt mRNA concentration (Figures 3J–3O). Importantly, *Porphyromonas*

**Figure 2. RORγt-Expressing Th17 Cells Protect against Glucose Intolerance**

(A) IPGTT was performed on 20-week-old WT (n = 5) and *RORγt*$^{-/-}$ (n = 3) mice fed with a NC; glycemic index (μM/min) was calculated.

(B) Plasma insulin was quantified by ELISA from fasted or fed 20-week-old *RORγt*$^{-/-}$ (n = 5) and WT (n = 6) mice.

(C) Glucose infusion rate (GIR) was calculated during a clamp in 20-week-old *RORγt*$^{-/-}$ (n = 8) and WT (n = 8) mice.

(D) Body weight gain of *RORγt*$^{-/-}$ (n = 3) and WT (n = 5) mice fed NC.

(E) Fat/lean ratio was calculated from EchoMRI analysis on 20-week-old *RORγt*$^{-/-}$ (n = 3) and WT (n = 5) mice.

(F) *RORγt*$^{-/-}$ (n = 6) and WT (n = 5) mice food intake was measured during 30 hr.

(G) IPGTT was performed on 12-week-old NC-fed WT (n = 5) and RORγt heterozygous (*RORγt*$^{+/-}$, n = 4) mice fed with a NC; glycemic index (μM/min) was calculated.

(H) Glucose infusion rate (GIR) was calculated during a clamp in *RORγt*$^{+/-}$ and WT mice, fed a NC (WT n = 6; *RORγt*$^{+/-}$ n = 5) or a HFD (WT n = 6; *RORγt*$^{+/-}$ n = 7) for 30 days.

(I) IPGTT was performed on HFD-fed (for 30 days) WT (n = 5) and *RORγt*$^{+/-}$ (n = 5) mice; glycemic index (μM/min) was calculated.

(J) Fat/lean ratio was calculated from EchoMRI analysis on *RORγt*$^{+/-}$ (NC n = 3; HFD n = 5) and WT (NC n = 5; HFD n = 5) mice after 30 days of HFD.

(K–P) Proportion of IL17 (K and N) and IFNγ (M and P)-producing CD4 T cells and Foxp3-expressing T cells (L and O) were analyzed by flow cytometry from SILP of WT, *RORγt*$^{-/-}$, and *RORγt*$^{+/-}$ mice fed a NC or a HFD (n = 5 mice/group).

(Q–Y) *Rag1*$^{-/-}$ mice were injected with T cells from *RORγt*$^{-/-}$ mice (*Rag1*$^{-/-}$ + LT *RORγt*$^{-/-}$) or WT mice (*Rag1*$^{-/-}$ + LT WT). (Q) Seven weeks after transfer, IPGTT was performed and glycemic index (μM/min) was calculated (n = 9 mice/group; data are from one experiment out of three). (R) GIR was calculated during a clamp procedure. (S) Plasma insulin was quantified from fasted or fed mice. (R and S) n = 5 mice/group; data are from one experiment out of two. (T–V) Phosphorylation of Akt (T) and GSK3 (U) was quantified by western blot in liver, EDL muscle, and soleus muscle at the end of the clamp (means ± SEM; n = 5 mice/group). (W) Body weight gain after T cell transfer expressed in %. (X) Fat/lean ratio was calculated from EchoMRI analysis. (Y) Food intake was measured over a 30 hr period. (X and Y) n = 5 mice/group; data are from one representative experiment out of two.

(A–Y) All values are means ± SEM; Different superscript letters (a, b) indicate data statistically different from each other with $p > 0.05$.

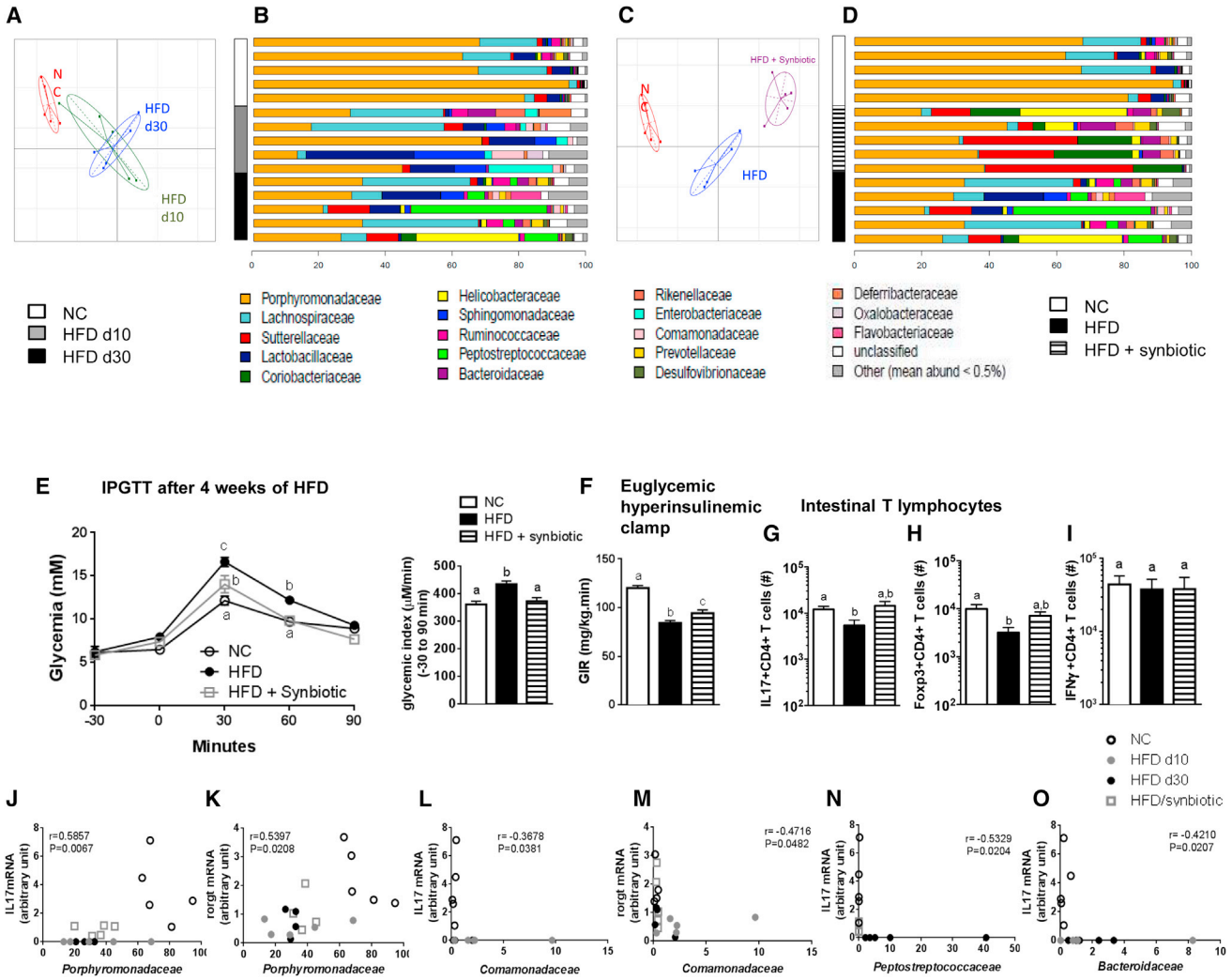


**Figure 3. The HFD Changes Ileum Mucosa Microbiota which Affects Intestinal Immunity**

(A and B) 16S rRNA gene sequencing analysis of the ileum mucosa microbiota from WT mice fed a NC (white squares) or a HFD for 10 (gray squares) or 30 days (black squares) (n = 5 mice/group): (A) Principal Coordinate Analysis (PCoA); (B) barplot analysis on family taxons. (C and I) WT mice were fed a NC (n = 5, white squares) or HFD and treated with saline (HFD, n = 5, black squares) or synbiotic (HFD + symbiotic, n = 5, hatch squares) for 30 days. (C and D) Ileum mucosa microbiota16S rRNA gene sequencing analysis: (C) PCoA, (D) barplot analysis on family taxons. (E) IPGTT was performed, and the glycemic index (µM/min) was calculated. (F) Glucose infusion rate (GIR) was calculated during a euglycemic hyperinsulinemic clamp. (G–I) Number of SILP IL17$^+$ (G), Foxp3$^+$ (H), and IFN$\gamma^+$ CD4 T cells (I) were determined by flow cytometry. (E–I) All values are ± SEM; one representative experiment out of two; different superscript letters (a, b, and c) indicate data statistically different from each other with $p > 0.05$. (J–O) Spearman correlation between *Porphyromonadaceae* (J and K), *Comamonadaceae* (L,M), *Peptostreptococcaceae* (N), *Bacteroidaceae* (O), and relative mRNA expression of IL17 (J, L, N, and O) or RORγt (K and M) in ileum mucosa of these mice.

*gengivalis*, a member of the *Porphyromonadaceae*, induces periodontitis (Grover et al., 2014) and triggers IL17 production (Takahashi et al., 2014). Therefore, this suggests that the reduction of *Porphyromonadaceae* in the ileum at the onset of disease could be responsible for the reduction of Th17 cells. Moreover, an increase of *Peptostreptococcaceae* is associated with the prevention from DSS-induced intestinal inflammation (Nagy-Szakal et al., 2013), which could also contribute to the decrease of Th17 cells.

Based on recent studies demonstrating that segmented filamentous bacteria (SFB) in the SI favor Th17 development (Gaboriau-Routhiau et al., 2009), we quantified the concentration of SFB by qPCR. We showed that SFB were much less abundant after 10 and 30 days on HFD than in the WT NC mice (Figure S5K). Their abundance was not restored by synbiotic treatment. There was a similar loss of SFB from *ROR*$\gamma t^{-/-}$ mice which was less pronounced in *ROR*$\gamma t^{+/-}$ mice (Figure S5K). Ivanov and colleagues (Ivanov et al., 2009) demonstrated that Th17 cell induction by SFB was due to the release of serum amyloid antigen (SAA) by DCs in the gut. Therefore, we assessed whether SAA levels in the ileum were affected in HFD-induced disease. SAA1, SAA2, and SAA3 mRNA levels decreased after 30 days on HFD when compared to NC-fed controls (Figures S5L–S5N). Thus, SFB and SAA are reduced in HFD-fed mice when compared to control mice, and this correlates with the loss of Th17 cells. Importantly, SAA3 was only restored by the

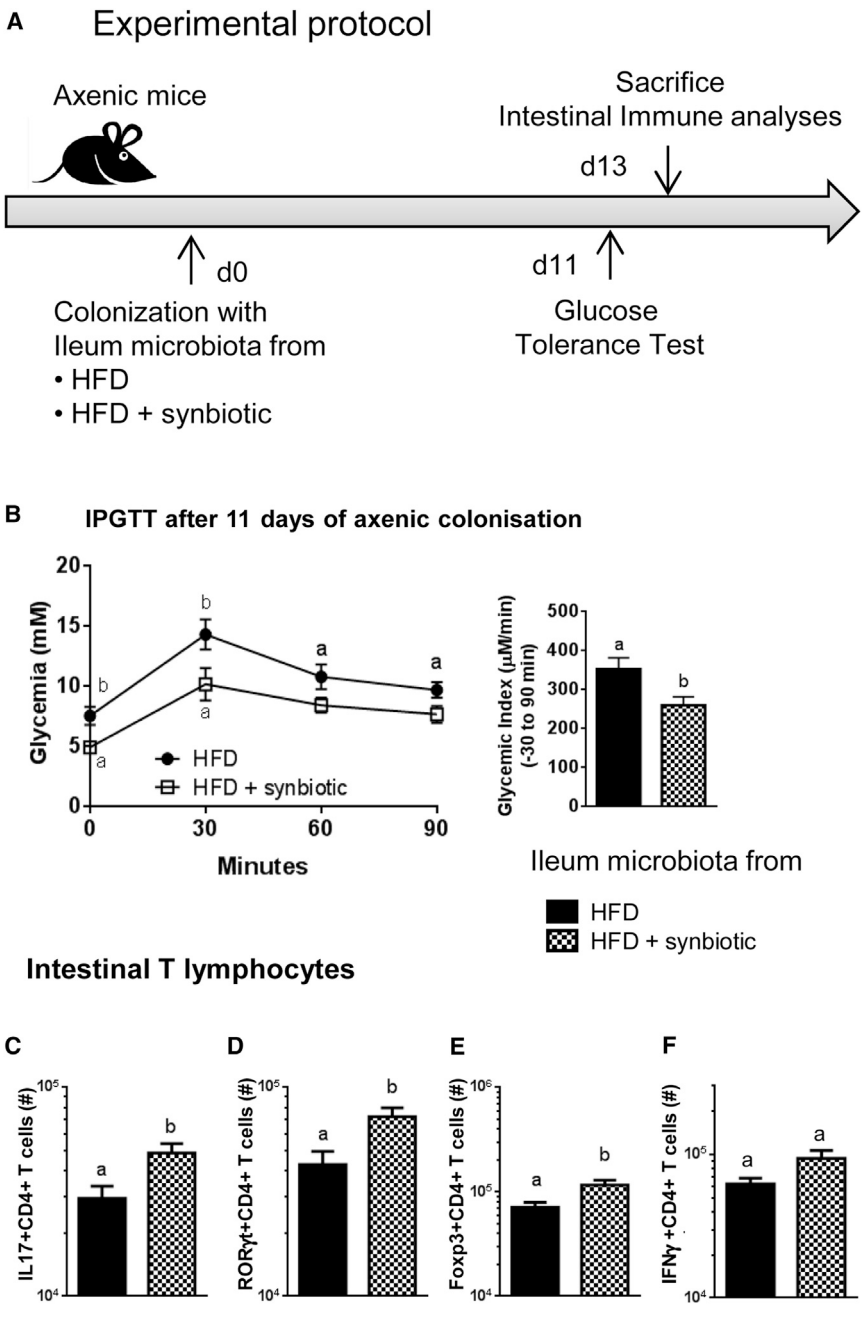


**Figure 4. Microbiota of Synbiotic Treated Mice Increases the Number of Intestinal RORγt-Th17 Cells and Prevents Glucose Intolerance**

(A) Experimental protocol: 12-week-old axenic mice were colonized with ileum microbiota from HFD mice (HFD; n = 7) or with HFD/synbiotic mice (HFD + synbiotic; n = 8).

(B) Eleven days after colonization (d11), IPGTT was performed and glycemic index (µM/min) was calculated.

(C–F) Numbers of SILP IL17$^+$ (C), RORγt$^+$ (D), Foxp3$^+$ (E), and IFNγ$^+$ CD4 T cells (F) were determined by flow cytometry. Graphs show means ± SEM; different superscript letters (a, b) indicate data statistically different from each other with $p > 0.05$.

synbiotic treatment, suggesting that it could rather be associated with the improved metabolic phenotype (Figures S5L–S5N).

To investigate whether HFD-induced changes in the gut microbiota are the direct cause of the decrease in ileum Th17 cells and metabolic disease, we colonized axenic mice with the ileum microbiota from HFD-fed mice treated or not with synbiotic for 30 days (Figure 4A). Mice colonized with the ileum microbiota from HFD-fed mice had higher fasting glycemia (7.5 mM) than those colonized with the microbiota from the HFD-fed mice given the synbiotic (4.9 mM) (Figure 4B), which was similar to that of conventional NC-fed mice (data not shown). Glucose tolerance was lower in the mice colonized with the microbiota from HFD-fed mice than in those colonized with HFD-fed synbiotic-treated microbiota (Figure 4B). The effect on the glucose tolerance was observed after only 2 weeks of colonization and associated with a decrease in the number of IL17/RORγt and Treg cells in the SILP (Figures 4C–4E). The number of Th1 cells was not statistically different in both groups (Figure 4F). The impact of the colonization with the ileum microbiota was specific to the SILP, since the number of Th17 and Treg cells were similar in the MLN from both groups of mice (data not shown). This supports the conclusion that these cells play a role at the onset of metabolic disease and that the intestinal microbiota is responsible for the changes in intestinal immunity observed in HFD-fed mice.

## The HFD Alters the Transcriptoms and Functions of Intestinal Defenses

Since the above evidences indicate that a decrease of SILP IL17/RORγt CD4 T cells contributes to the onset of metabolic disease, we investigated the mechanisms through which the HFD-induced changes in microbiota might cause the loss of Th17 cells. First, we analyzed the transcriptomic profiles of SILP CD4 T cells of NC and HFD-fed mice. Changes in the transcriptome of CD4 T cells were already evident after 10 days on HFD, and some of these differences were maintained up to 30 days; other changes appeared only after 30 days (Figure 5A). Hierarchical clustering analysis of the transcriptomic data was able to separate the gene expression profiles of CD4 T cells from mice fed a HFD for 10 and 30 days and those from NC fed mice (Figure 5A). The genes with altered expression at both 10 and 30 days on HFD were inflammatory genes *Ifng* and *Sap-kinase* (upregulated) and anti-inflammatory genes such as *Il27*, *Il18ra*, and *Il10* (downregulated). Two genes involved in CD4 T cell differentiation (*Foxp3*, *Gata3*) were downregulated (Figure S6A). Altogether,

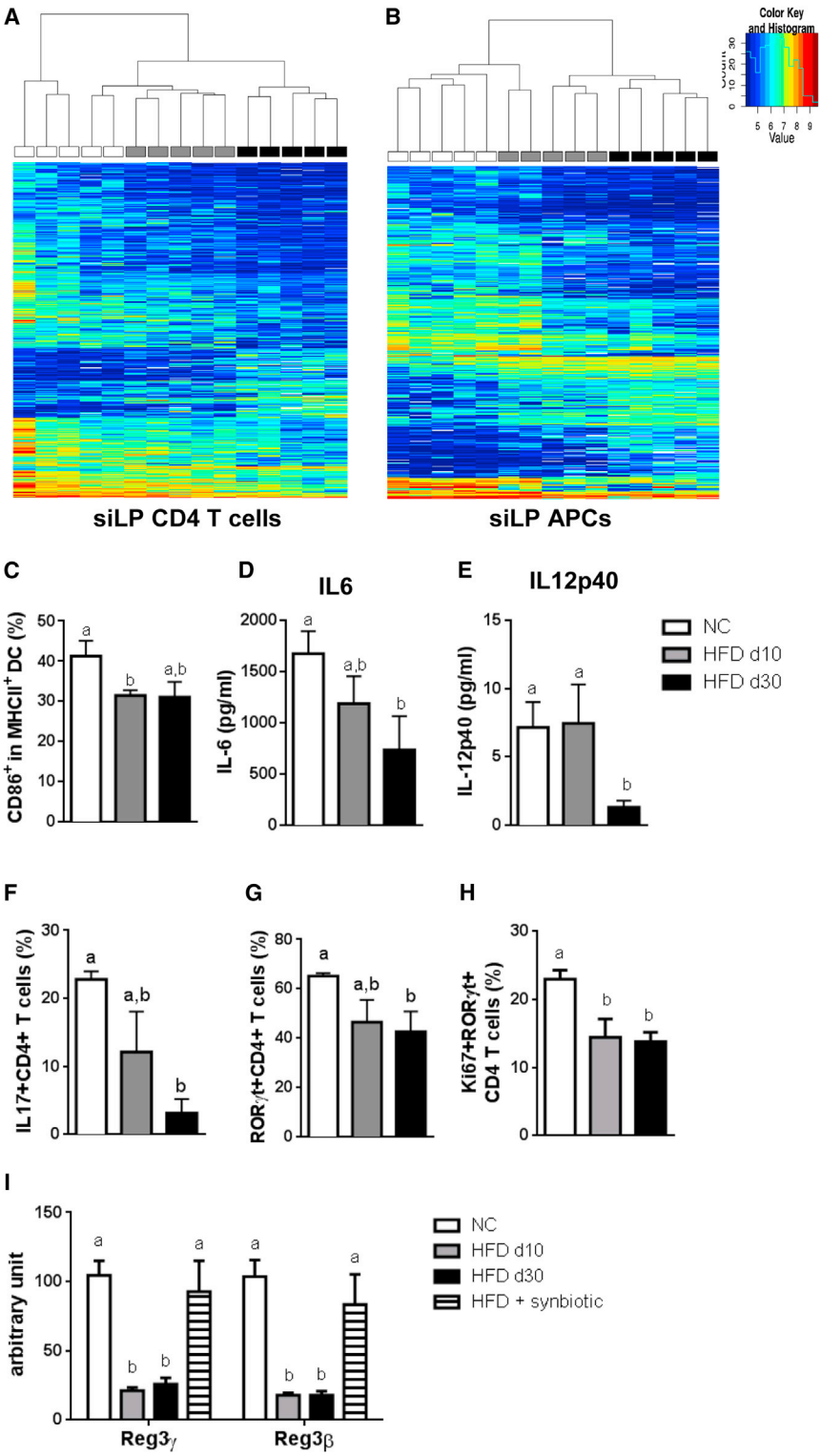


**Figure 5. The HFD Impairs the Gene Expression and the Function of SILP APCs to Promote Th17 Cell Differentiation**

(A and B) Transcriptional profiles of CD4 T cells (A) and APCs (B) from the SILP of NC mice (control; n = 10) or fed with a HFD for 10 (HFD d10; n = 10) or 30 days (HFD d30; n = 10), obtained by microarray analysis. Heatmaps show differential gene expression between HFD d10 versus NC and HFD d30 and NC (with $p > 0.05$). Hierarchical clustering shows the Euclidian distance between each point of SILP CD4 T cells (A) or APCs (B) (x axis) and between genes (y axis).

(C) Graphs show the % of CD86 on SILP DC from NC or HFD mice.

(D and E) Cytokine production by SILP leukocytes ($CD45^+$ cells) from mice fed a NC or a HFD IL6 (D) and IL12p40 (E) was assessed by ELISA.

(F and G) The % of $IL17^+$ (F) or $ROR\gamma t^+$ (G) OTII CD4 T cells after Th17 differentiation, with SILP cells from NC or HFD-fed mice were graphed.

(H) The proportion of SILP $TCR^+CD4^+ROR\gamma t^+$ cells expressing Ki67 in NC or HFD-fed mice was quantified.

(I) Quantification of Reg3β and Reg3γ mRNA by RT-qPCR of ileum from mice fed a NC, HFD d10 or HFD d30, and synbiotic-treated HFD mice (HFD + synbiotic).

(C–I) Graphs values are means ± SEM; n = 5 mice/group; one representative experiment out of two; different superscript letters (a, b) indicate data statistically different from each other with $p > 0.05$.

these data confirmed that HFD modified the intestinal CD4 T cell expression profile. Since the gut microbiota regulates intestinal immune homeostasis (Mortha et al., 2014), at least in part, through the differentiation of Th17 cells in the SILP in an SFB and APC-dependent manner (Goto et al., 2014), we analyzed the transcriptomic profiles of SILP APCs which revealed broad differences in gene expression between all groups (Figure 5B). Hierarchical clustering analysis of the data distinguished the expression profiles of APCs from mice fed a NC from those of HFD-fed mice (Figure 5B). Further analyses of the expression of genes in APCs from mice fed a HFD for 10 or 30 days revealed upregulation of the expression of some genes implicated in inflammatory pathways *Nfkb1*, *Nfx1*, *Nlrp3*, *IL6st*, and *Thbs* and of genes involved in the cell stress response *psmc4*, *H2-1b*, *ffar2,3,6*, and *niacr1*, when compared to those of NC-fed mice (Figure S6B). We also analyzed genes involved in T cell costimulation and found that *icam1* and *cd86* were downregulated (Figure S6B). These changes in expression of *icam1* and *cd86* were confirmed by RT-qPCR of ileum mRNA (Figures S6C and S6D). We also found less IL12p40 mRNA in the ileum of mice after 10 and 30 days on HFD when compared to NC mice (Figure S6E). To further analyze whether the changes in mRNA levels were associated with changes in protein concentrations, we characterized the different subsets of SILP APCs. Their numbers were unchanged,

and neither dendritic cells nor macrophages were statistically affected (Figures S6F–S6J). A decrease expression of the CD86 protein was seen by flow cytometry in SILP APCs after 10 and 30 days on HFD (Figure 5C). In light of the changes in gene expression observed in APCs, we then evaluated their ability to produce IL6 and IL12p40 (cytokines produced by APCs), required for the differentiation and maintenance of Th17 cells, in response to LPS in vitro. The SILP leukocytes from mice fed a HFD for 30 days produced less IL6 and IL12p40 than NC controls (Figures 5D and 5E). This impaired cytokine production was SILP specific, since no major changes were observed in leukocytes from the MLN (Figures S6K and S6L) or from the IEL (data not shown). We next evaluated the ability of SILP APCs from NC or HFD-fed mice to induce Th17 cell differentiation. Naive CD4 T cells were cultured with SILP APCs from NC and HFD-fed mice and with a Th17-inducing cocktail. SILP leukocytes of mice fed a HFD for 10 or 30 days were less able to induce Th17 cells (IL17/RORγt CD4 T cells) than those from NC mice (Figures 5F and 5G). Moreover, the proportion of proliferating (Ki67+) IL17/RORγt CD4 T cells in vivo, in the SILP, in mice after 10 or 30 days on HFD was lower than in NC mice (Figure 5H). Overall, these data show that the HFD impaired the ability of APCs to promote Th17 cell differentiation in the ileum. In contrast to the SILP leukocytes, those isolated from the MLN after 10 or 30 days on HFD induced more RORγt CD4 T cells and had no effect on IL-17 production when compared to those from NC mice (Figures S6M and S6N). Similarly, there was no difference between the proportion of proliferating IL17/RORγt CD4 T cells in vivo in the MLN from NC and HFD-fed mice (Figure S6O).

Altogether, our data suggest that the loss of Th17 cells in metabolic disease is due to an impaired APC function in the SILP following HFD-induced changes in the microbiota. This process would lead to a leaky gut. Further investigations are needed to identify bacteria functions and the corresponding mechanisms responsible for the decrease of intestinal Th17.

In order to evaluate the importance of the decrease of Th17 cells on the intestinal nonspecific defense (Ishigame et al., 2009) during metabolic disease, we quantified mRNA level of antimicrobial peptides Reg3β and Reg3γ which are involved in the mucosal protection. Reg3β and Reg3γ were decreased after 10 days on HFD and remained at a low level after 30 days on HFD (Figure 5I). Synbiotic treatment prevented the decrease of both (Figure 5I). Since metabolic disease is associated with increased gut permeability characterized by an increased bacterial translocation (Amar et al., 2011), we sequenced the 16S rRNA gene in the MAT and found that the bacterial taxons present in HFD mice were dramatically different from those of NC. This tissue microbiota dysbiosis induced by HFD in the MAT (Figures 6A and 6B) and liver (data not shown) is associated with a moderate accumulation of Th17 cells in the liver and MAT. This could be explained by Th17 cell migration from the SILP toward the liver and or MAT, thereby reducing the number of Th17 cells in the intestine. However, this hypothesis is unlikely, since it has been reported that the migration of T cells from the specific site of antigen sensitization toward nondraining tissues was not associated, conversely to what we observed, with a reduction in the number of T cells at the site of antigen sensitization (Ruane et al., 2013). A most likely hypothesis is that a change in tissue microbiota could be responsible for the recruitment of newly activated infiltrating Th17 cells, as shown elsewhere (Bertola et al., 2012), to trigger metabolic inflammation. In addition, this tissue dysbiosis was prevented by the synbiotic treatment (Figures 6A and 6B). Importantly, this feature was most likely linked to the reduced IL17/RORγt CD4 T cells induced by the HFD, since it was also observed in *RORγt*$^{-/-}$ mice (Figures 6C and 6D) and in *RORγt*$^{-/-}$ T cells transferred to Rag1 mice (Figures 6E and 6F). Our result is supported by reports showing a loss of IL22-producing CD4 T cells in HIV-infected human subjects (Page et al., 2014) associated with an increased bacterial translocation (Mavigner et al., 2012), since these patients also have a higher incidence of T2D and lipodystrophy (Samaras, 2012).

Altogether, our findings provide the basis for a model in which a fat-enriched diet results in specific changes in the gut microbiota that consequently impair the immune system of the SI by affecting the function of APCs in the differentiation of intestinal RORγt/Th17 cells (i.e., Th17 cells). This impaired intestinal vigilance early in the course of metabolic disease leads to a change in tissue microbiota, contributing to a later state of systemic low-grade inflammation. This concept could provide new opportunities for the prevention and treatment of metabolic disease, including the development of treatments that may be restricted to the intestine to avoid broad systemic deleterious effects.

## EXPERIMENTAL PROCEDURES

### Animal Models

Eight-week-old WT male mice were fed with a NC diet or a HFD (72%) or a high-fat high-carbohydrate diet (HFHCD) (45%) for 30 days. For the synbiotic treatment, mice were gavaged with polydextrose PDX with *Bifidobacterium lactis* B420 (kindly provided by DuPont Nutrition & Health) or with saline for the controls. Twelve-week-old male axenic C57Bl/6 mice were colonized with the ileum content. Mouse genotype and diet information are reported in Supplemental Information. All of the animal experimental procedures were validated by the local ethical committee of the Rangueil Hospital.

### RNA Extraction and Quantification

All tissues were homogenized in TRIzol (Life Technologies) and extracted. q-PCR reactions were performed on a ViiA7 Real-Time PCR System (Life Technologies). Data were analyzed with the ViiA7 RUO Real-Time PCR analysis software. Primer sequences are reported in Supplemental Information.

### Ileum Mucosa and Adipose Tissue 16S rRNA Sequencing Analysis

The microbial population present in ileum and adipose tissue has been determined using generation high throughput sequencing of variable regions of the 16S rRNA bacterial gene (Vaiomer SAS, Labège, France). PCR amplification was performed using 16S universal primers targeting the V3-V4 region. The detection of the sequencing fragments was performed using MiSeq Illumina technology. More details are reported in Supplemental Information. NCBI SRA bioproject was SUB949277 PRJNA284574.

### Monitoring Metabolic Parameters

Glucose tolerance test was performed by intraperitoneal injection of glucose (IPGTT). The glycemic index was calculated by adding the glycemic values from all time points multiplied by the duration of the test. Plasma insulin concentration was assessed by ELISA (Mercodia kit). Euglycemic hyperinsulinemic clamps were performed at a rate of 18 mU.kg$^{-1}$.min$^{-1}$ of insulin. Body mass composition was analyzed by quantitative nuclear magnetic resonance (EchoMRI-100TM). For food, intake was measured during 30 hr. More details are reported in Supplemental Information.

### Liver and MAT Leukocyte Isolation

Liver (Garidou et al., 2009) and MAT (Luche et al., 2013) infiltrating leukocytes were isolated as previously described. Liver and MAT leukocyte isolation is described in detail in the Supplemental Information.

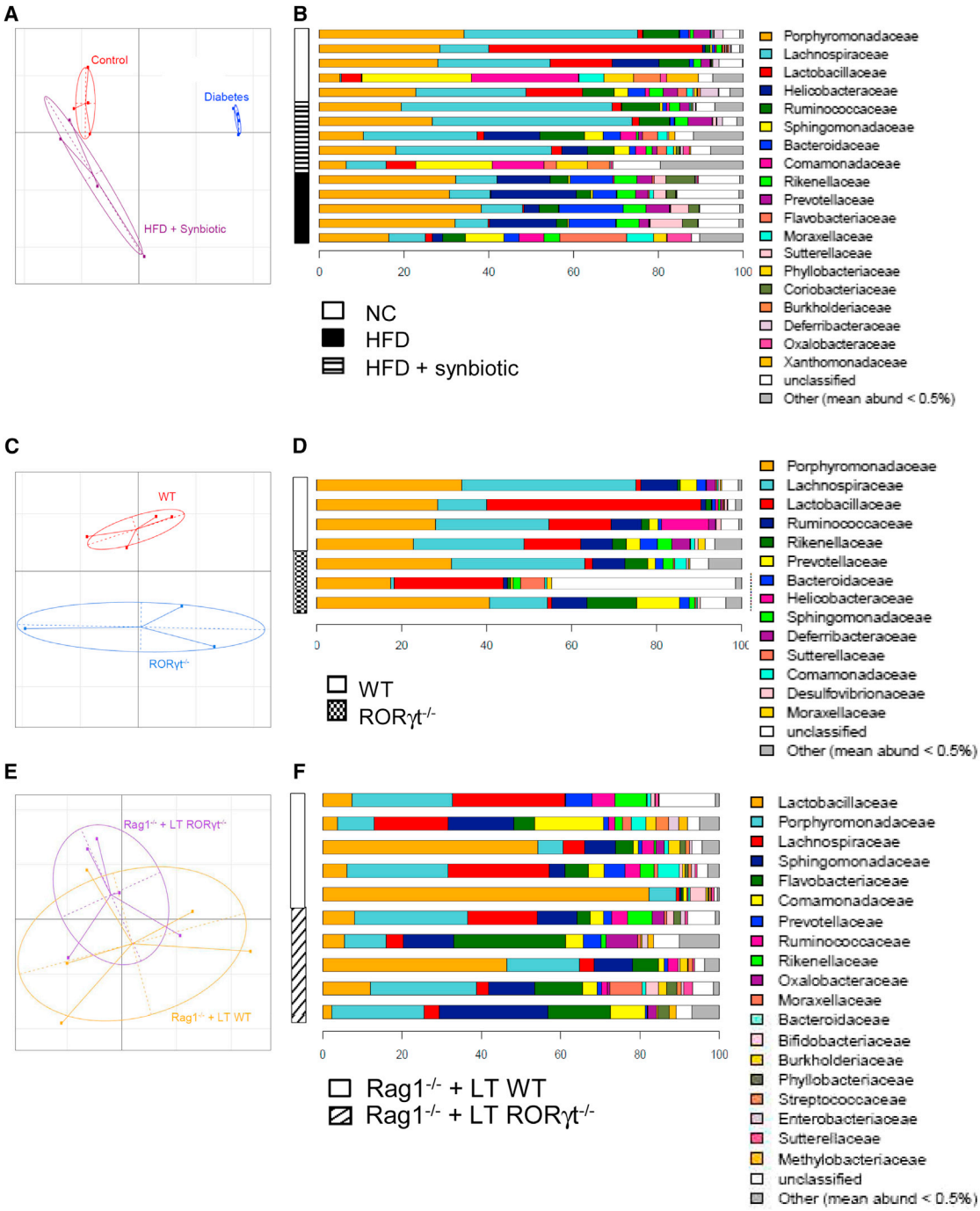


**Figure 6. Intestinal Immunity Alteration Is Associated with Changes in Tissue Microbiota**

16S rRNA gene sequencing analysis of the MAT microbiota from (A and B) NC-fed mice (white squares), fed a HFD for 30 days (HFD) (black squares) and synbiotic treated HFD mice (HFD + symbiotic, hatch squares) (n = 5 mice/group); (C and D) NC-fed WT (n = 5, white squares) and *RORγt*$^{-/-}$ (n = 3, hatch squares) mice; (E and F) *Rag1*$^{-/-}$ mice injected with WT T cells (*Rag1*$^{-/-}$ + LT WT; n = 5 [white squares]) or with *RORγt*$^{-/-}$ T cells (*Rag1*$^{-/-}$ + LT RORγt; n = 5 [hatched squares]): (A, C, and E) PCoA; (B, D, and F) barplot analysis on family taxons.

### MLN and Intestinal Leukocytes Isolation

MLN and SI were harvested and Peyer's patches were dissected from the SI segments. To isolate IEL, SI was incubated with EDTA. Subsequently, fragments were incubated with collagenase and DNase to isolate leukocytes (SILPs). The SILPs were harvested from the 70%–40% Percoll interface. For MLN and Peyer's patches, single-cell suspensions were prepared by mechanically disrupting. Isolation procedures are described in Supplemental Information.

### Flow Cytometry

For surface staining experiments, leukocyte suspensions were labeled with antibodies anti-F4/80, MHCII, CD4, CD8, CD11b, CD86, TCR,

CD19, CD45, and CD11c. Cells were also stained with the LIVE/DEAD Fixable Cell Stain Kit (Life Technologies). Then cells were fixed, permeabilized, and labeled with monoclonal antibodies anti-Foxp3, RORγt, Ki67.

For intracellular cytokine analyses, immune cells were stimulated (Maret et al., 2003) and stained on the surface as described above. They were fixed, permeabilized, and labeled with anti-IFNγ and IL17. The labeled cell suspension was analyzed using a digital flow cytometer (LSR II Fortessa) and FlowJo software (Tree Star). Details about antibody and labeling procedure are reported in Supplemental Information.

### T Cell Isolation for Adoptive Transfer

T cells were isolated from WT or *RORγt*$^{-/-}$ mice, and 5 × 10$^6$ cells were injected into *Rag1*$^{-/-}$ mice.

### Detection of Cytokines by ELISA

SILP or MLN cells were stimulated with LPS. IL-6, IL-12p40 concentrations in supernatants were determined by ELISA. More details are reported in Supplemental Information.

### In Vitro Th17 Differentiation

Splenic naive CD4 T cells were isolated from OTII and cultured with irradiated MLN or SILP leukocytes with OVA peptide and a Th17 differentiation cocktail for 5 days. IL17+ and RORγt+ CD4 T cells were analyzed by cytometry as described above, and more details are provided in Supplemental Information.

### Western Blot Analysis

Protein of liver and muscles were separated on gel electrophoresis, transferred onto membrane (GE Healthcare), and hybridized with antibodies against pAkt, Akt, pNFκB p65, NFκB p65, pGSK-3β, GSK-3β, and GAPDH. Immunoblots were revealed by enhanced chemiluminescence (BIO-RAD). Antibody references are reported in Supplemental Information.

### Microarray Analysis of Intestinal CD4$^+$ T Cells and APCs

CD4$^+$ T cells and APCs from the SILP were sorted (Influx, Becton Dickinson). RNA was extracted, amplified and expression profiling was performed by Miltenyi Genomic Services (Miltenyi Biotec, Paris, France) using the Agilent Microarray (Miltenyi Biotec). More details are provided in Supplemental Information.

### Data Analysis

Data were analyzed by using Microsoft Excel, and graphs were done by GraphPad Prism. Statistical significance ($p < 0.05$) was determined by using a Student's t test, Mann-Whitney, Kruskal-W.

## ACCESSION NUMBERS

NCBI GEO accession numbers are as follows: GSE52557, GSE52558, GSE52559.

## SUPPLEMENTAL INFORMATION

Supplemental Information includes six figures and Supplemental Experimental Procedures and can be found with this article at http://dx.doi.org/10.1016/j.cmet.2015.06.001.

## AUTHOR CONTRIBUTIONS

L.G., C.P., and R.B. designed the experiments. L.G., C.P., P.K., A.W., J.C., M.A., A.G., C.D., J.S.I., B.L., F.S., and C.H. produced the data. L.G., C.P., and R.B. wrote the manuscript. M.S., L.S., S.L., M.C., X.C., J.A., P.V., G.E., and N.F. edited the manuscript. G.E. provided mice and edited the manuscript. L.G. started the project, and L.G. and C.P. designed, performed, and analyzed experiments.

## CONFLICT OF INTEREST

R.B. and J.A. are shareholders of Vaiomer. R.B. and J.A. are founders of Vaiomer and members of its scientific advisory board. M.C. is an employee and shareholder of Vaiomer.

## ACKNOWLEDGMENTS

R.B. is a recipient of grants from the 7th European Framework Program (Florinash), the *Agence Nationale de la Recherche* (ANR; Floradip, Transflora, Bactimmunodia), and the *Société Francophone de Diabétologie* (SFD). L.G. and V.D.-E. are recipients of grants from the European Association for the Study of Diabetes. We thank J.-J. Maoret and F. Martins from the Quantitative Transcriptomic Facility (I2MC Inserm/UPS UMR1048), the team from the Genomic/Sequencing Facility (UMR5165 CNRS/UPS–UDEAR), and A. Zakaroff and C. Pecher from the flow cytometry facility (I2MC Inserm/UPS UMR1048). We also thank Y. Barreira and her team from the Animal Care Facility of Rangueil Hospital (UMS US006/Inserm). Drs. Carol Featherstone and Jeffrey Christensen helped us to prepare this manuscript. Finally, we thank Dr. Sophie Laffont-Pradines for helpful discussions. We also thank Anthony Puel and Vincent Azalbert.

Received: September 10, 2014
Revised: March 31, 2015
Accepted: June 2, 2015
Published: July 7, 2015

## REFERENCES

Amar, J., Chabo, C., Waget, A., Klopp, P., Vachoux, C., Bermúdez-Humarán, L.G., Smirnova, N., Bergé, M., Sulpice, T., Lahtinen, S., et al. (2011). Intestinal mucosal adherence and translocation of commensal bacteria at the early onset of type 2 diabetes: molecular mechanisms and probiotic treatment. EMBO Mol. Med. *3*, 559–572.

Atarashi, K., Tanoue, T., Shima, T., Imaoka, A., Kuwahara, T., Momose, Y., Cheng, G., Yamasaki, S., Saito, T., Ohba, Y., et al. (2011). Induction of colonic regulatory T cells by indigenous Clostridium species. Science *331*, 337–341.

Bäckhed, F., Ding, H., Wang, T., Hooper, L.V., Koh, G.Y., Nagy, A., Semenkovich, C.F., and Gordon, J.I. (2004). The gut microbiota as an environmental factor that regulates fat storage. Proc. Natl. Acad. Sci. USA *101*, 15718–15723.

Bertola, A., Ciucci, T., Rousseau, D., Bourlier, V., Duffaut, C., Bonnafous, S., Blin-Wakkach, C., Anty, R., Iannelli, A., Gugenheim, J., et al. (2012). Identification of adipose tissue dendritic cells correlated with obesity-associated insulin-resistance and inducing Th17 responses in mice and patients. Diabetes *61*, 2238–2247.

Bleau, C., Karelis, A.D., St-Pierre, D.H., and Lamontagne, L. (2014). Crosstalk between intestinal microbiota, adipose tissue and skeletal muscle as an early event in systemic low-grade inflammation and the development of obesity and diabetes. Diabetes Metab. Res. Rev. http://dx.doi.org/10.1002/dmrr.2617.

Bollrath, J., and Powrie, F.M. (2013). Controlling the frontier: regulatory T-cells and intestinal homeostasis. Semin. Immunol. *25*, 352–357.

Brown, K., DeCoffe, D., Molcan, E., and Gibson, D.L. (2012). Diet-induced dysbiosis of the intestinal microbiota and the effects on immunity and disease. Nutrients *4*, 1095–1119.

Burcelin, R., Crivelli, V., Dacosta, A., Roy-Tirelli, A., and Thorens, B. (2002). Heterogeneous metabolic adaptation of C57BL/6J mice to high-fat diet. Am. J. Physiol. Endocrinol. Metab. *282*, E834–E842.

Cani, P.D., Bibiloni, R., Knauf, C., Waget, A., Neyrinck, A.M., Delzenne, N.M., and Burcelin, R. (2008). Changes in gut microbiota control metabolic endotoxemia-induced inflammation in high-fat diet-induced obesity and diabetes in mice. Diabetes *57*, 1470–1481.

Chewning, J.H., and Weaver, C.T. (2014). Development and survival of Th17 cells within the intestines: the influence of microbiome- and diet-derived signals. J. Immunol. *193*, 4769–4777.

Feuerer, M., Herrero, L., Cipolletta, D., Naaz, A., Wong, J., Nayer, A., Lee, J., Goldfine, A.B., Benoist, C., Shoelson, S., and Mathis, D. (2009). Lean, but

not obese, fat is enriched for a unique population of regulatory T cells that affect metabolic parameters. Nat. Med. *15*, 930–939.

Gaboriau-Routhiau, V., Rakotobe, S., Lécuyer, E., Mulder, I., Lan, A., Bridonneau, C., Rochet, V., Pisi, A., De Paepe, M., Brandi, G., et al. (2009). The key role of segmented filamentous bacteria in the coordinated maturation of gut helper T cell responses. Immunity *31*, 677–689.

Garidou, L., Heydari, S., Truong, P., Brooks, D.G., and McGavern, D.B. (2009). Therapeutic memory T cells require costimulation for effective clearance of a persistent viral infection. J. Virol. *83*, 8905–8915.

Goto, Y., Panea, C., Nakato, G., Cebula, A., Lee, C., Diez, M.G., Laufer, T.M., Ignatowicz, L., and Ivanov, I.I. (2014). Segmented filamentous bacteria antigens presented by intestinal dendritic cells drive mucosal Th17 cell differentiation. Immunity *40*, 594–607.

Grover, V., Kapoor, A., Malhotra, R., and Kaur, G. (2014). Porphyromonas gingivalis antigenic determinants–potential targets for the vaccine development against periodontitis. Infect. Disord. Drug Targets *14*, 1–13.

Hooper, L.V., and Gordon, J.I. (2001). Commensal host-bacterial relationships in the gut. Science *292*, 1115–1118.

Hotamisligil, G.S. (2006). Inflammation and metabolic disorders. Nature *444*, 860–867.

Ishigame, H., Kakuta, S., Nagai, T., Kadoki, M., Nambu, A., Komiyama, Y., Fujikado, N., Tanahashi, Y., Akitsu, A., Kotaki, H., et al. (2009). Differential roles of interleukin-17A and -17F in host defense against mucoepithelial bacterial infection and allergic responses. Immunity *30*, 108–119.

Ivanov, I.I., and Littman, D.R. (2011). Modulation of immune homeostasis by commensal bacteria. Curr. Opin. Microbiol. *14*, 106–114.

Ivanov, I.I., McKenzie, B.S., Zhou, L., Tadokoro, C.E., Lepelley, A., Lafaille, J.J., Cua, D.J., and Littman, D.R. (2006). The orphan nuclear receptor RORgammat directs the differentiation program of proinflammatory IL-17+ T helper cells. Cell *126*, 1121–1133.

Ivanov, I.I., Atarashi, K., Manel, N., Brodie, E.L., Shima, T., Karaoz, U., Wei, D., Goldfarb, K.C., Santee, C.A., Lynch, S.V., et al. (2009). Induction of intestinal Th17 cells by segmented filamentous bacteria. Cell *139*, 485–498.

Kang, H.S., Okamoto, K., Kim, Y.S., Takeda, Y., Bortner, C.D., Dang, H., Wada, T., Xie, W., Yang, X.P., Liao, G., and Jetten, A.M. (2011). Nuclear orphan receptor TAK1/TR4-deficient mice are protected against obesity-linked inflammation, hepatic steatosis, and insulin resistance. Diabetes *60*, 177–188.

Khovidhunkit, S.O., Suwantuntula, T., Thaweboon, S., Mitrirattanakul, S., Chomkhakhai, U., and Khovidhunkit, W. (2009). Xerostomia, hyposalivation, and oral microbiota in type 2 diabetic patients: a preliminary study. J. Med. Assoc. Thai. *92*, 1220–1228.

Kolida, S., and Gibson, G.R. (2011). Synbiotics in health and disease. Annu. Rev. Food Sci. Technol. *2*, 373–393.

Konieczna, P., Ferstl, R., Ziegler, M., Frei, R., Nehrbass, D., Lauener, R.P., Akdis, C.A., and O'Mahony, L. (2013). Immunomodulation by Bifidobacterium infantis 35624 in the murine lamina propria requires retinoic acid-dependent and independent mechanisms. PLoS ONE *8*, e62617.

Lefèvre, L., Galès, A., Olagnier, D., Bernad, J., Perez, L., Burcelin, R., Valentin, A., Auwerx, J., Pipy, B., and Coste, A. (2010). PPARγ ligands switched high fat diet-induced macrophage M2b polarization toward M2a thereby improving intestinal Candida elimination. PLoS ONE *5*, e12828.

Littman, D.R., and Rudensky, A.Y. (2010). Th17 and regulatory T cells in mediating and restraining inflammation. Cell *140*, 845–858.

Lochner, M., Ohnmacht, C., Presley, L., Bruhns, P., Si-Tahar, M., Sawa, S., and Eberl, G. (2011). Microbiota-induced tertiary lymphoid tissues aggravate inflammatory disease in the absence of RORgamma t and LTi cells. J. Exp. Med. *208*, 125–134.

Luche, E., Cousin, B., Garidou, L., Serino, M., Waget, A., Barreau, C., André, M., Valet, P., Courtney, M., Casteilla, L., and Burcelin, R. (2013). Metabolic endotoxemia directly increases the proliferation of adipocyte precursors at the onset of metabolic diseases through a CD14-dependent mechanism. Mol. Metab. *2*, 281–291.

Luck, H., Tsai, S., Chung, J., Clemente-Casares, X., Ghazarian, M., Revelo, X.S., Lei, H., Luk, C.T., Shi, S.Y., Surendra, A., et al. (2015). Regulation of obesity-related insulin resistance with gut anti-inflammatory agents. Cell Metab. *21*, 527–542.

Lutsey, P.L., Pankow, J.S., Bertoni, A.G., Szklo, M., and Folsom, A.R. (2009). Serological evidence of infections and Type 2 diabetes: the MultiEthnic Study of Atherosclerosis. Diabet. Med. *26*, 149–152.

Macêdo, D.P., Oliveira, N.T., Farias, A.M., Silva, V.K., Wilheim, A.B., Couto, F.M., and Neves, R.P. (2010). Esophagitis caused by Candida guilliermondii in diabetes mellitus: first reported case. Med. Mycol. *48*, 862–865.

Maret, A., Coudert, J.D., Garidou, L., Foucras, G., Gourdy, P., Krust, A., Dupont, S., Chambon, P., Druet, P., Bayard, F., and Guéry, J.C. (2003). Estradiol enhances primary antigen-specific CD4 T cell responses and Th1 development in vivo. Essential role of estrogen receptor alpha expression in hematopoietic cells. Eur. J. Immunol. *33*, 512–521.

Mavigner, M., Cazabat, M., Dubois, M., L'Faqihi, F.E., Requena, M., Pasquier, C., Klopp, P., Amar, J., Alric, L., Barange, K., et al. (2012). Altered CD4+ T cell homing to the gut impairs mucosal immune reconstitution in treated HIV-infected individuals. J. Clin. Invest. *122*, 62–69.

Mortha, A., Chudnovskiy, A., Hashimoto, D., Bogunovic, M., Spencer, S.P., Belkaid, Y., and Merad, M. (2014). Microbiota-dependent crosstalk between macrophages and ILC3 promotes intestinal homeostasis. Science *343*, 1249288.

Nagy-Szakal, D., Hollister, E.B., Luna, R.A., Szigeti, R., Tatevian, N., Smith, C.W., Versalovic, J., and Kellermayer, R. (2013). Cellulose supplementation early in life ameliorates colitis in adult mice. PLoS ONE *8*, e56685.

Nishimura, S., Manabe, I., Nagasaki, M., Eto, K., Yamashita, H., Ohsugi, M., Otsu, M., Hara, K., Ueki, K., Sugiura, S., et al. (2009). CD8+ effector T cells contribute to macrophage recruitment and adipose tissue inflammation in obesity. Nat. Med. *15*, 914–920.

Page, E.E., Greathead, L., Metcalf, R., Clark, S.A., Hart, M., Fuchs, D., Pantelidis, P., Gotch, F., Pozniak, A., Nelson, M., et al. (2014). Loss of Th22 cells is associated with increased immune activation and IDO-1 activity in HIV-1 infection. J. Acquir. Immune Defic. Syndr. *67*, 227–235.

Round, J.L., and Mazmanian, S.K. (2010). Inducible Foxp3+ regulatory T-cell development by a commensal bacterium of the intestinal microbiota. Proc. Natl. Acad. Sci. USA *107*, 12204–12209.

Ruane, D., Brane, L., Reis, B.S., Cheong, C., Poles, J., Do, Y., Zhu, H., Velinzon, K., Choi, J.H., Studt, N., et al. (2013). Lung dendritic cells induce migration of protective T cells to the gastrointestinal tract. J. Exp. Med. *210*, 1871–1888.

Samaras, K. (2012). The burden of diabetes and hyperlipidemia in treated HIV infection and approaches for cardiometabolic care. Curr. HIV/AIDS Rep. *9*, 206–217.

Shale, M., Schiering, C., and Powrie, F. (2013). CD4(+) T-cell subsets in intestinal inflammation. Immunol. Rev. *252*, 164–182.

Sommer, F., and Bäckhed, F. (2013). The gut microbiota–masters of host development and physiology. Nat. Rev. Microbiol. *11*, 227–238.

Takahashi, S., Fukuda, M., Mitani, A., Fujimura, T., Iwamura, Y., Sato, S., Kubo, T., Sugita, Y., Maeda, H., Shinomura, T., and Noguchi, T. (2014). Follicular dendritic cell-secreted protein is decreased in experimental periodontitis concurrently with the increase of interleukin-17 expression and the Rankl/Opg mRNA ratio. J. Periodontal Res. *49*, 390–397.

Turnbaugh, P.J., Ley, R.E., Mahowald, M.A., Magrini, V., Mardis, E.R., and Gordon, J.I. (2006). An obesity-associated gut microbiome with increased capacity for energy harvest. Nature *444*, 1027–1031.

Wang, X., Ota, N., Manzanillo, P., Kates, L., Zavala-Solorio, J., Eidenschenk, C., Zhang, J., Lesch, J., Lee, W.P., Ross, J., et al. (2014). Interleukin-22 alleviates metabolic disorders and restores mucosal immunity in diabetes. Nature *514*, 237–241.

Weisberg, S.P., McCann, D., Desai, M., Rosenbaum, M., Leibel, R.L., and Ferrante, A.W., Jr. (2003). Obesity is associated with macrophage accumulation in adipose tissue. J. Clin. Invest. *112*, 1796–1808.

Winer, D.A., Winer, S., Shen, L., Wadia, P.P., Yantha, J., Paltser, G., Tsui, H., Wu, P., Davidson, M.G., Alonso, M.N., et al. (2011). B cells promote insulin resistance through modulation of T cells and production of pathogenic IgG antibodies. Nat. Med. *17*, 610–617.